Energy Management of a Parallel Hybrid Electric Vehicle Equipped with a Voltage Booster

Souad Hadj-Said, Guillaume Colin, Ahmed Ketfi-Cherif, Yann Chamaillard

Energy Management of a Parallel Hybrid Electric Vehicle Equipped with a Voltage Booster

S. Hadj-Said *,** **G. Colin** ** **A. Ketfi-Cherif** *
Y. Chamaillard **

* *Renault S.A.S, France (e-mail: souad.hadj-said@renault.com ; ahmed.ketfi-cherif@renault.com).*
** *Univ. Orléans, PRISME, EA 4229, F45072, Orléans, France (e-mail: guillaume.colin@univ-orleans.fr ; yann.chamaillard@univ-orleans.fr)*

Abstract: In this paper, the optimization problem of energy management for a parallel hybrid electric vehicle equipped with a Step-Up converter is resolved analytically using Pontryagin's Maximum Principle (PMP). The analytical method is based on convex models, which are identified from the reference models. A numerical method based on the reference models is also used in order to validate the analytical method by comparing their results. In this work, two optimization variables are considered: the power split between the Internal Combustion Engine (ICE) and the Electric Machine (EM) and the output voltage of the booster. The simulation results show that the analytical approach reduces considerably the computing time and has an very low suboptimality comparing to the numerical method.

Keywords: Energy Management Strategy, Hybrid Electric Vehicles (HEV), Step-Up Converter, Analytical Method, Convex optimization, Pontryagin's Maximum Principle (PMP).

1. INTRODUCTION

The continued increase of vehicles number in the world poses two major issues: energy and pollution. This is why, the automotive manufacturers design hybrid vehicles in order to reduce energy consumption and pollution emissions. The study presented in this paper focuses on the energy management of Hybrid Electric Vehicles (HEV). The energy management consists of calculating optimal controls that minimize the energy consumption. The studied vehicle is composed of an Internal Combustion Engine (ICE), one or more Electric Machines (EM), and a battery. This energy storage element delivers a continuous and almost constant voltage. Depending on the need, the adaptation of the electric energy between the battery and the EM is ensured by electric converters, among them the Step-Up which is a DC/DC converter. The role of the Step-up is to boost the battery voltage in order to increase the EM performance. The losses produced by the electric components depend strongly on the output Step-Up voltage. This is why we propose to control the voltage to minimize the electric consumption.

There are many approaches to design an optimal energy management strategy (Zhang et al., 2015), the most known are: deterministic Dynamic Programming (DP) (Pérez et al., 2006; Debert et al., 2010), stochastic DP (Johannesson et al., 2007; Asher et al., 2017), and Pontryagin's Maximum Principle (PMP) (Serrao et al., 2009; Kim et al., 2011; Stockar et al., 2011; Ahmadizadeh et al., 2017). While it can potentially give the globally optimal energy management, dynamic programming is computationally expensive, which limits its application to low-order systems (typically two states). The PMP offers the possibility to compact the optimization problem by defining the Hamiltonian function to handle the balance between the fuel cost and other related constraints, typically the battery state of charge. However, the main difficulty of the PMP method remains in finding the co-state.

The PMP method is widely used in this area, both analytically and numerically. In Hadj-Said et al. (2017), we proposed an analytical method to optimize power split and gear box using PMP. In the latter, we used a linear electric model while in this paper the electric model is quadratic. In Elbert et al. (2014) and Ambühl et al. (2010), the optimal torque split and the engine state On/Off were computed analytically using the PMP approach for a serial hybrid electric bus. Pham et al. (2016) proposed to calculate in addition the optimal EM On/Off analytically using the PMP, while in Nüesch et al. (2014), the engine On/Off and gearshift stategies were given numerically by a combination of DP and PMP. In this study, the main contributions are: finding the optimal power split and the output Step-Up voltage analytically using PMP.

Concerning the voltage optimization, in Toshifumi Yamakawa (2011), the inventors proposed to implement a voltage setting map as a function of the rotational speed and the torque of the EM composed by two regions: a non-boost region and a boost region. These regions were determined by minimizing the EM losses.

The main objectives of this paper is to find an energy management solution that minimizes the energy consumed by the vehicle. An analytical solution, based on PMP, is proposed for energy management of a parallel HEV.

This paper is organized as follows. In section 2, the reference and the analytical models are presented. In section 3, the off-line resolution of the optimization problem is proposed in two steps: first, the optimal power and then the voltage. In section 4, the implementation of the analytical solutions is presented. Finally, the simulation results obtained analytically in the MIL (Model In the Loop) are compared to the results obtained numerically in section 5. The purpose of this comparison is to validate the analytical solutions.

2. MODELING

As shown in Fig.1, the HEV consists of a battery, a Step-Up, an electric motor (EM), and an ICE delivering power to the wheels via a gearbox.

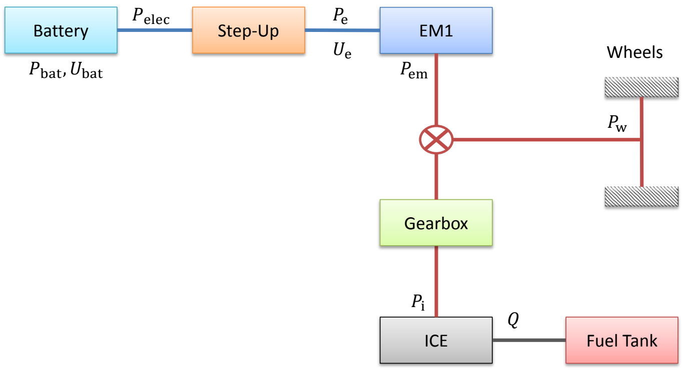

Fig. 1. HEV Powertrain

The wheel power $P_{\rm w}$, demanded by the driver, is calculated from the vehicle speed set-point. So, the vehicle speed is considered as an input of the optimization, and is given by different cycles. The optimization variables are the output step-up voltage $U_{\rm e}$ and the mechanical power of the electric machine $P_{\rm em}$.

2.1 Vehicle Model

The vehicle dynamics are governed by the following equations:

$$F_{\rm w}(t) = m_{\rm vec}\dot{v}(t) + F_{\rm res}(t)[N] \quad (1)$$

$$T_{\rm w}(t) = F_{\rm w}(t).R_{\rm w}[N.m] \quad (2)$$

$$\omega_{\rm w}(t) = \frac{v(t)}{R_{\rm w}}[rad/s] \quad (3)$$

$$P_{\rm w}(t) = T_{\rm w}(t)\omega_{\rm w}(t)[W] \quad (4)$$

where $F_{\rm w}$ is the force at the wheels, $F_{\rm res}(t) = F_{\rm tires} + F_{\rm aero}(t)$ the resistive force which includes the aerodynamic force ($F_{\rm aero}(t) = 0.5.\rho.S.Cx.v^2(t)$) and the tire resistance ($F_{\rm tires}$, here assumed constant), $m_{\rm vec}[kg]$ the total vehicle mass and $R_{\rm w}[m]$ the wheel radius. $P_{\rm w}$, $T_{\rm w}$ and $\omega_{\rm w}$ are the power, the torque and the rotational speed of the wheels.

The relation between the rotational speed and those of the engine ($\omega_{\rm i}$) and the EM ($\omega_{\rm e}$) is given by:

$$\omega_{\rm i}(t) = \omega_{\rm w}(t)R_{\rm Gear}(t) \quad (5)$$

$$\omega_{\rm e}(t) = \omega_{\rm w}(t)R_{\rm EM} \quad (6)$$

where $R_{\rm EM}$ and $R_{\rm Gear}$ are respectively the electric ratio and the gear ratio which are determined in advance of optimization.

2.2 Reference Model

Engine The engine is modeled by its fuel consumption to deliver the mechanical power $P_{\rm i}$. This consumption is expressed by the fuel flow (Q).

$$Q(t) = \dot{m}_{\rm fuel}(T_{\rm i}(t), \omega_{\rm i}(t)) \; [g/s] \quad (7)$$

where $\dot{m}_{\rm fuel}(T_{\rm i}(t), \omega_{\rm i}(t))$ is the fuel consumption map and $T_{\rm i}$ is the engine torque. The mechanical power generated by the engine is expressed by: $P_{\rm i} = T_{\rm i}\omega_{\rm i}$ $[W]$ and limited by two functions of $\omega_{\rm i}$:

$$\underline{P}_{\rm i}(\omega_{\rm i}(t)) \leq P_{\rm i}(t) \leq \overline{P}_{\rm i}(\omega_{\rm i}(t)) \quad (8)$$

Electric Motor The electric motor model expresses the electric power produced by the EM which includes the mechanical power delivered and the losses obtained from the specific power loss of the EM. So, the electric power $P_{\rm e}$ has the following expression:

$$P_{\rm e}(t) = P_{\rm em}(t) + loss(T_{\rm e}(t), \omega_{\rm e}(t), U_{\rm e}(t)) \; [W] \quad (9)$$

where $loss(T_{\rm e}(t), \omega_{\rm e}(t), U_{\rm e}(t))$ is the electric motor losses map and $T_{\rm e}$ is the EM torque. The mechanical power generated by the EM is expressed by: $P_{\rm em}(t) = T_{\rm e}(t)\omega_{\rm e}(t)$ $[W]$ and limited by two functions of $\omega_{\rm e}$ and $U_{\rm e}$:

$$\underline{P}_{\rm e}(\omega_{\rm e}(t), U_{\rm e}(t)) \leq P_{\rm em}(t) \leq \overline{P}_{\rm e}(\omega_{\rm e}(t), U_{\rm e}(t)) \quad (10)$$

Step-Up The Step-Up is modeled by its losses ($P_{\rm S}$). They are expressed with respect to the electric power produced by the electric motors, the battery voltage, and the output voltage of the Step-up. In a step-up there are losses caused by conduction ($P_{\rm Conduction}$) as well as losses caused by switching of diodes and IGBT ($P_{\rm Switching}$). Therefore, $P_{\rm S}$ are given by (Badin, 2013):

$$P_{\rm S}(i_{\rm bat}, U_{\rm e}) = P_{\rm Conduction} + P_{\rm Switching}[W] \quad (11)$$

$P_{\rm Conduction}$ is given by:

$$P_{\rm Conduction} = (R_{\rm Coil} + rR_{\rm IGBT} + (1-r)R_{\rm Diode})i_{\rm bat}^2 \quad (12)$$

where $R_{\rm Coil}$ is the coil resistance, $R_{\rm IGBT}$ is the IGBT resistance, $R_{\rm Diode}$ is the diode resistance and r is the duty cycle defined by:

$$r = \frac{U_{\rm e} - U_{\rm bat}}{U_{\rm e}}$$

$P_{\rm Switching}$ is given by:

$$P_{\rm Switching} = V_0 U_{\rm e} i_{\rm bat} + (rV_{\rm IGBT} + (1-r)V_{\rm Diode})i_{\rm bat} \quad (13)$$

where $V_{\rm IGBT}$ is the IGBT voltage, and $V_{\rm Diode}$ is the diode voltage.

When $U_{\rm e} = U_{\rm bat}$, $P_{\rm Switching} = 0$ and $P_{\rm Conduction}$ is given by:

$$P_{\rm Conduction} = \begin{cases} (R_{\rm Coil} + R_{\rm Diode})i_{\rm bat}^2 & \text{if } P_{\rm elec} \geq 0 \\ (R_{\rm Coil} + R_{\rm IGBT})i_{\rm bat}^2 & \text{if } P_{\rm elec} < 0 \end{cases}$$

$P_{\rm S}$ can take the following general form regarding $i_{\rm bat}$:

$$P_{\rm S}(i_{\rm bat}, U_{\rm e}) = U_{\rm S}(U_{\rm e})i_{\rm bat} + R_{\rm S}i_{\rm bat}^2 \quad (14)$$

where, $R_{\rm S} = R_{\rm Coil} + (1-r)R_{\rm Diode} + rR_{\rm IGBT}$

Battery The battery is modeled as a resistive circuit (Badin, 2013; Murgovski et al., 2012) and the battery power is given by:

$$P_{\text{bat}}(t) = OCV(SoC)i_{\text{bat}}(t)[W] \tag{15}$$

$$P_{\text{bat}}(t) = P_{\text{elec}}(t) + R_{\text{bat}}(SoC)i^2_{\text{bat}}(t) \tag{16}$$

$$P_{\text{elec}}(t) = P_{\text{e}}(t) + P_{\text{S}}(t) \tag{17}$$

By inserting (17) and (14) in (15), i_{bat} is calculated as follows:

$$i_{\text{bat}}(t) = \frac{U_{\text{tot}} - \sqrt{U^2_{\text{tot}} - 4R_{\text{tot}}P_{\text{e}}}}{2R_{\text{tot}}} \tag{18}$$

where $U_{\text{tot}} = OCV(SoC) - U_{\text{S}}(U_{\text{e}})$ and $R_{\text{tot}} = R_{\text{S}} + R_{\text{bat}}$. The State of Charge ($SoC$) of the battery is defined as:

$$\dot{SoC}(t) = -\frac{i_{\text{bat}}(t)}{Q_{max}} \tag{19}$$

where $Q_{max}[C]$ is the maximum battery charge.

2.3 Convex Model

Some assumptions and approximations were made to make the models convex.

Engine The fuel flow Q is modeled by the "Willans Lines Model" as described in Rizzoni et al. (1999). Its analytical model is given by:

$$Q(P_{\text{i}}) = \begin{cases} a_1 P_{\text{i}} + Q_0 & \text{if } \underline{P}_{\text{i}} \le P_{\text{i}} \le P_{\text{lim}} \\ a_2(P_{\text{i}} - P_{\text{lim}}) + Q_{\text{lim}} & \text{if } P_{\text{lim}} \le P_{\text{i}} \le \overline{P}_{\text{i}} \end{cases} \tag{20}$$

where Q_0 is the idle fuel consumption. The parameters Q_0, P_{lim} and Q_{lim} depend on ω_{i}, while, a_1, a_2 are assumed constant, where $a_1 << a_2$. Fig. 2 shows that the approximated engine model is sufficiently representative of the reference engine model. $RMSE_{\text{fuel}}$ is the Root Mean Square Error between the reference model (7) and the convex model (20).

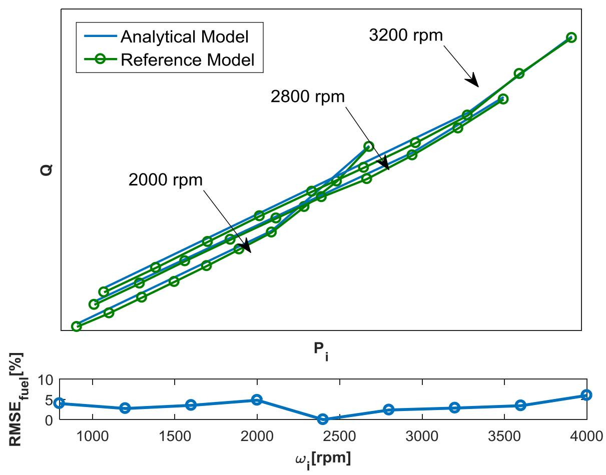

Fig. 2. Validation of the convex model of $Q[g.s^{-1}]$ in function of $P_{\text{i}}[W]$ (axes have been removed for confidentiality reasons)

EM, Battery, and Step-Up Concerning the electrical part, it is assumed that the open circuit voltage (OCV) is constant in the definition set of SoE. Therefore, the State of Energy (SoE) can be used instead of SoC as:

$$\dot{SoE}(t) = -\frac{OCV i_{\text{bat}}(t)}{E_{max}} = -\frac{P_{\text{bat}}(t)}{E_{max}} \tag{21}$$

where $E_{max} = OCVQ_{max}[J]$ is the maximal battery energy. The $SoE[\%]$ is limited by:

$$20 \le SoE(t) \le 80 \tag{22}$$

The analytical model of the battery power is given by:

$$P_{\text{bat}}(T_{\text{e}}, \omega_{\text{e}}, U_{\text{e}}) = \begin{cases} a^- P^2_{\text{em}} + b^- P_{\text{em}} + c \text{ if } \underline{P}_{\text{e}} \le P_{\text{em}} \le 0 \\ a^+ P^2_{\text{em}} + b^+ P_{\text{em}} + c \text{ if } 0 \le P_{\text{em}} \le \overline{P}_{\text{e}} \end{cases} \tag{23}$$

where, $a^\pm$, $b^\pm$ and c are modeled as following:

$$a^\pm(\omega_{\text{e}}, U_{\text{e}}) = \frac{\sum_{m=0}^2 \sum_{l=0}^2 \alpha^\pm_{ml} U^l_{\text{e}} \omega^m_{\text{e}}}{\omega^2_{\text{e}}} \tag{24}$$

$$b^\pm(\omega_{\text{e}}, U_{\text{e}}) = \frac{\sum_{m=0}^2 \sum_{l=0}^2 \beta^\pm_{ml} U^l_{\text{e}} \omega^m_{\text{e}}}{\omega_{\text{e}}} \tag{25}$$

$$c(\omega_{\text{e}}, U_{\text{e}}) = \sum_{m=0}^{2} \sum_{l=0}^{2} \gamma_{ml} U^l_{\text{e}} \omega^m_{\text{e}} \tag{26}$$

The P_{bat} model has been validated as shown in Fig. 3. Where, $RMSE_{\text{EM}}$ is the root mean square error between the reference model (15) and the convex model (23).

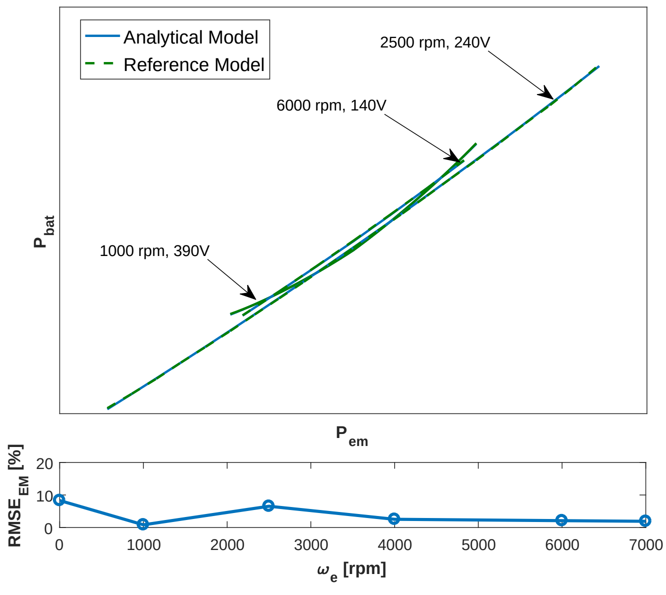

Fig. 3. Validation of the convex model of $P_{\text{bat}}[W]$ in function of $P_{\text{em}}[W]$ (axes have been removed for confidentiality reasons)

3. OFF-LINE OPTIMIZATION

In this section, the off-line optimization is presented. It is recalled that the rotational speeds ω_{i} and ω_{e} are determined from (5) and (6).

3.1 Power Split Optimization

Here, to optimize the EM power (P_{em}), we assume that the output Step-Up voltage U_{e} is known. In a parallel HEV, ICE and EM are mechanically connected to the wheels, therefore:

$$P_{\text{w}}(t) = P_{\text{em}}(t) + P_{\text{i}}(t) \tag{27}$$

The Power Optimization Problem (POP) to determine $P_{\text{em}}^{\text{opt}}$ is formulated as:

$$POP : \begin{cases} \min_{P_{\text{em}}} \; J \\ \dot{SoE}(t) = -\frac{P_{\text{bat}}(P_{\text{em}}(t))}{E_{max}} \\ 0 \leq SoE(t) \leq 100 \\ P_{\text{i}} + P_{\text{em}} = P_{\text{w}} \\ \underline{P}_{\text{i}}(\omega_{\text{i}}, P_{\text{w}}) \leq P_{\text{i}}(t) \leq \overline{P}_{\text{i}}(\omega_{\text{i}}, P_{\text{w}}) \\ \underline{P}_{\text{e}}(\omega_{\text{e}}, U_{\text{e}}, P_{\text{w}}) \leq P_{\text{em}}(t) \leq \overline{P}_{\text{e}}(\omega_{\text{e}}, U_{\text{e}}, P_{\text{w}}) \end{cases} \tag{28}$$

where:

$$J = \int_{t_0}^{t_f} Q(P_{\text{i}}(t), \omega_{\text{i}}(t))dt \tag{29}$$

SoE is the state, P_{em} is the control, and from (27) we obtain:

$$\underline{P}_{\text{i}}(\omega_{\text{i}}, P_{\text{w}}) = \max(\underline{P}_{\text{i}}(\omega_{\text{i}}), P_{\text{w}} - \overline{P}_{\text{e}}(\omega_{\text{e}}, U_{\text{e}}))$$
$$\overline{P}_{\text{i}}(\omega_{\text{i}}, P_{\text{w}}) = \min(\overline{P}_{\text{i}}(\omega_{\text{i}}), P_{\text{w}} - \underline{P}_{\text{e}}(\omega_{\text{e}}, U_{\text{e}}))$$
$$\underline{P}_{\text{e}}(\omega_{\text{e}}, U_{\text{e}}, P_{\text{w}}) = \max(\underline{P}_{\text{e}}(\omega_{\text{e}}, U_{\text{e}}), P_{\text{w}} - \overline{P}_{\text{i}}(\omega_{\text{i}}))$$
$$\overline{P}_{\text{e}}(\omega_{\text{e}}, U_{\text{e}}, P_{\text{w}}) = \min(\overline{P}_{\text{e}}(\omega_{\text{e}}, U_{\text{e}}), P_{\text{w}} - \underline{P}_{\text{i}}(\omega_{\text{i}}))$$

To find the optimal power, the PMP is used. So, according to the PMP, minimizing J is equivalent to minimizing the Hamiltonian function which is calculated from (20) and (23), as follows:

$$H_{\text{hyb}}(P_{\text{i}}, P_{\text{em}}, P_{\text{w}}, \lambda) = Q(P_{\text{i}}) + \lambda(t)(P_{\text{bat}}(P_{\text{em}})) \tag{30}$$

where λ is the Langrange Factor.

The Hamiltonian function H_{hyb} is the sum of two piecewise functions. So, to find $P_{\text{em}}^{\text{opt}}$, first, we have to calculate the expression of H_{hyb}. This is done by considering the points where the functions Q and P_{bat} change their coefficients. These points are: $P_{\text{em}} = P_{\text{w}} - P_{\text{lim}}$ and $P_{\text{em}} = 0$. They are called here: "The Particular Points".

The general expression of H_{hyb} is:

$$H_{\text{hyb}}(P_{\text{em}}) = A_1(P_{\text{w}} - P_{\text{em}}) + A_0 + \lambda(B_2 P_{\text{em}}^2 + B_1 P_{\text{em}} + B_0)$$

A_1, A_0, B_2, B_1 and B_0 are determined, according to (20), (23) and (27), as follows:

- $P_{\text{em}} > P_{\text{w}} - P_{\text{lim}}$ then $A_0 = Q_0$, $A_1 = a_1$
- $P_{\text{em}} < P_{\text{w}} - P_{\text{lim}}$ then $A_0 = Q_{\text{lim}} - a_2 P_{\text{lim}}$, $A_1 = a_2$
- $P_{\text{em}} > 0$ then $B_1 = b^+$, $B_2 = a^+$
- $P_{\text{em}} < 0$ then $B_1 = b^-$, $B_2 = a^-$

Since H_{hyb} is convex, the optimum P_{em}^* is the solution of the following equation:

$$\frac{\partial H_{\text{hyb}}}{\partial P_{\text{em}}} = 0 \tag{31}$$

Then,

$$P_{\text{em}}^* = \frac{A_1 - \lambda B_1}{2\lambda B_2}$$

But H_{hyb} is a piecewise function then P_{em}^* should be compared to the particular points to determine A_1, B_1 and B_2. In addition, P_{em}^* must be in the admissible set $[\underline{P}_{\text{e}}(P_{\text{w}}), \overline{P}_{\text{e}}(P_{\text{w}})]$. Therefore, the following equations are studied regarding P_{w} and λ:

(a) $P_{\text{em}}^* = \overline{P}_{\text{e}}(P_{\text{w}}) \Leftrightarrow \lambda = \lambda_1 = \frac{A_1}{B_1 + 2B_2\overline{P}_{\text{e}}(P_{\text{w}})}$
(b) $P_{\text{em}}^* = (P_{\text{w}} - P_{\text{lim}}) \Leftrightarrow \lambda = \lambda_2 = \frac{A_1}{B_1 + 2B_2(P_{\text{w}} - P_{\text{lim}})}$
(c) $P_{\text{em}}^* = 0 \Leftrightarrow \lambda = \lambda_0 = \frac{A_1}{B_1}$
(d) $P_{\text{em}}^* = \underline{P}_{\text{e}}(P_{\text{w}}) \Leftrightarrow \lambda = \lambda_3 = \frac{A_1}{B_1 + 2B_2\underline{P}_{\text{e}}(P_{\text{w}})}$

We can note that the particular factors λ_0, λ_1, λ_2 and λ_3 depend on P_{w}. Therefore, the optimal solution $P_{\text{em}}^{\text{opt}}$ is calculated for all the admissible set: $P_{\text{w}} \in [\underline{P}_{\text{w}}, \overline{P}_{\text{w}}]$, where $\underline{P}_{\text{w}} = \underline{P}_{\text{i}}(\omega_{\text{i}}) + \underline{P}_{\text{e}}(\omega_{\text{e}}, U_{\text{e}})$ and $\overline{P}_{\text{w}} = \overline{P}_{\text{i}}(\omega_{\text{i}}) + \overline{P}_{\text{e}}(\omega_{\text{e}}, U_{\text{e}})$. For instance, if $P_{\text{w}} < \underline{P}_{\text{i}} \Rightarrow P_{\text{em}} < 0 \Rightarrow B_1 = b^-$, $B_2 = a^-$. And if $P_{\text{w}} - P_{\text{lim}} > \underline{P}_{\text{e}}$ then $\forall P_{\text{w}} \in [P_{\text{lim}} + \underline{P}_{\text{e}}, \underline{P}_{\text{i}}]$, $P_{\text{em}}^{\text{opt}}$ is given as shown in the table of Fig. 4.

λ	0	λ_1	λ_{21}	λ_{22}	λ_3	$+\infty$
$P_{\text{em}}^{\text{opt}}$	$\overline{P}_{\text{e}}$	$\frac{a_1 - \lambda b^-}{2\lambda a^-}$	$P_{\text{w}} - P_{\text{lim}}$	$\frac{a_2 - \lambda b^-}{2\lambda a^-}$	$\underline{P}_{\text{e}}$	

Fig. 4. An example of $P_{\text{em}}^{\text{opt}}$ according to P_{w} and λ

where, $\lambda_1 = \frac{a_1}{b^- + 2a^- \overline{P}_{\text{e}}}$, $\lambda_{21} = \frac{a_1}{b^- + 2a^-(P_{\text{w}} - P_{\text{lim}})}$, $\lambda_{22} = \frac{a_2}{b^- + 2a^-(P_{\text{w}} - P_{\text{lim}})}$, $\lambda_3 = \frac{a_2}{b^- + 2a^- \underline{P}_{\text{e}}}$.

3.2 Voltage Optimization

In this section, the optimization of the output Step-Up voltage will be presented. Here, we assume that the electric torque T_{e} is known. The PMP method is applied to solve the Voltage Optimization Problem (VOP):

$$VOP : \begin{cases} \min_{U_{\text{e}}} \; H_{\text{hyb}}(P_{\text{i}}, P_{\text{em}}, U_{\text{e}}, \lambda) \\ \dot{SoE}(t) = -\frac{P_{\text{bat}}(P_{\text{em}}, U_{\text{e}})}{E_{max}} \\ 0 \leq SoE(t) \leq 100 \\ U_{\text{e}} \in [U_{\text{bat}}, \overline{U}_{\text{e}}] \end{cases} \tag{32}$$

where the Hamiltonian function is given as:

$$H_{\text{hyb}}(P_{\text{i}}, P_{\text{em}}, U_{\text{e}}, \lambda) = Q(P_{\text{i}}) + \lambda P_{\text{bat}}(P_{\text{em}}, U_{\text{e}})$$

We can note that Q does not depend on U_{e}, therefore:

$$U_{\text{e}}^{\text{opt}} = \arg\min_{U_{\text{e}}} H_{\text{hyb}} = \arg\min_{U_{\text{e}}} P_{\text{bat}}$$

So, to find $U_{\text{e}}^{\text{opt}}$, we must solve the following equation:

$$\frac{\partial P_{\text{bat}}}{\partial U_{\text{e}}} = 0$$

According to (23), P_{bat} can be written in the following form:

$$P_{\text{bat}}(T_{\text{e}}, \omega_{\text{e}}, U_{\text{e}}) = U_2(T_{\text{e}}, \omega_{\text{e}})U_{\text{e}}^2 + U_1(T_{\text{e}}, \omega_{\text{e}})U_{\text{e}} + U_0(T_{\text{e}}, \omega_{\text{e}}) \tag{33}$$

Then, $\frac{\partial P_{\text{bat}}}{\partial U_{\text{e}}} = 0 \Leftrightarrow U_{\text{e}}^*(T_{\text{e}}, \omega_{\text{e}}) = \frac{-U_1(T_{\text{e}}, \omega_{\text{e}})}{2U_2(T_{\text{e}}, \omega_{\text{e}})}$

where:

$$U_2(T_{\text{e}}, \omega_{\text{e}}) = \begin{cases} \sum_{m=0}^{2} (\alpha_{m2}^- T_{\text{e}}^2 + \beta_{m2}^- T_{\text{e}} + \gamma_{m2})\omega_{\text{e}}^m & \text{if } T_{\text{e}} \leq 0 \\ \sum_{m=0}^{2} (\alpha_{m2}^+ T_{\text{e}}^2 + \beta_{m2}^+ T_{\text{e}} + \gamma_{m2})\omega_{\text{e}}^m & \text{if } T_{\text{e}} \geq 0 \end{cases}$$

$$U_1(T_\mathrm{e},\omega_\mathrm{e}) = \begin{cases} \sum_{m=0}^{2}(\alpha_{m1}^{-}T_\mathrm{e}^2+\beta_{m1}^{-}T_\mathrm{e}+\gamma_{m1})\omega_\mathrm{e}^m & \text{if } T_\mathrm{e}\le 0 \\ \sum_{m=0}^{2}(\alpha_{m1}^{+}T_\mathrm{e}^2+\beta_{m1}^{+}T_\mathrm{e}+\gamma_{m1})\omega_\mathrm{e}^m & \text{if } T_\mathrm{e}\ge 0 \end{cases}$$

Finally, since $U_2(T_\mathrm{e},\omega_\mathrm{e}) > 0\ \forall\ T_\mathrm{e},\omega_\mathrm{e}$, $U_\mathrm{e}^{\mathrm{opt}}$ is given as a function of T_e and ω_e (Fig. 5), by:

$$U_\mathrm{e}^{\mathrm{opt}} = \begin{cases} U_\mathrm{bat} & \text{if} \quad U_\mathrm{e}^*(T_\mathrm{e},\omega_\mathrm{e}) \le U_\mathrm{bat} \\ U_\mathrm{e}^*(T_\mathrm{e},\omega_\mathrm{e}) & \text{if } U_\mathrm{bat} \le U_\mathrm{e}^*(T_\mathrm{e},\omega_\mathrm{e}) \le \overline{U}_\mathrm{e} \\ \overline{U}_\mathrm{e} & \text{if} \quad U_\mathrm{e}^*(T_\mathrm{e},\omega_\mathrm{e}) \ge \overline{U}_\mathrm{e} \end{cases} \quad (34)$$

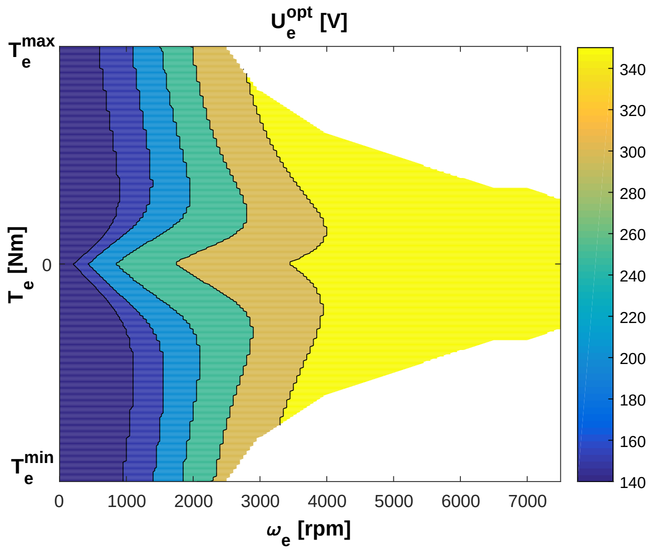

Fig. 5. The optimal Voltage regarding T_e and ω_e (the torque axe has been removed for confidentiality reasons)

4. ON-LINE OPTIMIZATION

This section descibes how the analytical and numerical approaches are implemented in the Model In Loop (MIL) structure.

Fig. 6 shows the on-line optimization process in the MIL. Actually, by taking into account the engine, the EM and the Step-Up dynamics, at an instant t, the power optimization receives the current voltage $U_\mathrm{e}^{\mathrm{c}}$, while the voltage optimization takes the current electric torque $T_\mathrm{e}^{\mathrm{c}}$.

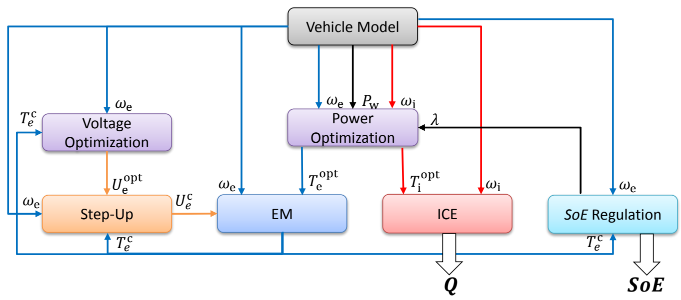

Fig. 6. On-Line Optimization for a Parallel HEV

For the optimal power, as shown in Fig.4, $P_\mathrm{em}^{\mathrm{opt}}$ is implemented in the form of tables regarding P_w and λ. Then, at an instant t, the expression of $P_\mathrm{em}^{\mathrm{opt}}$ is found by placing $P_\mathrm{w}(t)$ and $\lambda(t)$ with respect to their intervals. Concerning the voltage U_e, the optimal solution given in (34) is implemented.

The co-state λ is derterminded by a PID regulator of the *SoE*.

The diagram in Fig.7 explains the numerical approach to resolve *POP* and *VOP* by applying PMP and using the reference models. First, at every instant t, the controls P_em and U_e are meshed from their minimum to their maximum. Then, the numerical value of H_hyb is calculated using the complete models of Q and P_bat (given in (20), (23), (16) and (11)). Finally, the optimal control $P_\mathrm{em}^{\mathrm{opt}}, U_\mathrm{e}^{\mathrm{opt}}$ is the one which corresponds to the minimum value of H_hyb. In this approach, the optimality of $U_\mathrm{e}^{\mathrm{opt}}$ and $P_\mathrm{em}^{\mathrm{opt}}$ depends on the meshing. This is why the numerical method was tested in simulation for a meshing of 10 points (called "Num_1" in section 5) and 100 points (called "Num_2" in section 5) .

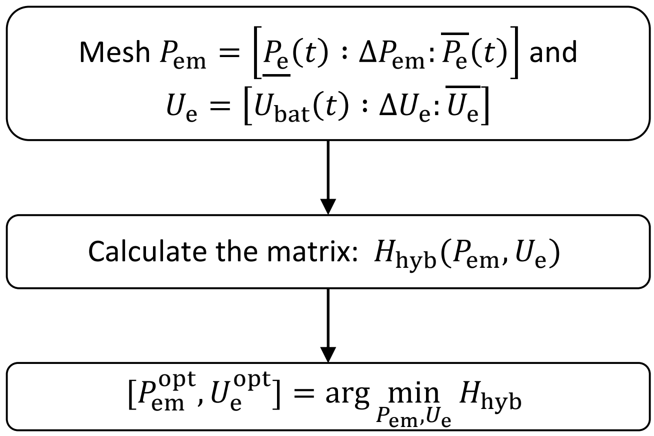

Fig. 7. Implementation of the numerical method

5. SIMULATION RESULTS

In this section, the fuel consumption and SoE trajectory results of the analytical method are compared to those of the numerical method in order to establish the performances of the analytical method. The fuel consumption (FC) and the electric losses (EL) are obtained by applying the strategies on the reference models.

Table 1 shows that the analytical method has almost the same fuel and electric consumptions as the ones found by the numerical methods for all studied cycles. For the urban driving, the analytical mehtod is better than "Num_1". In addition, the average values of the Computing Time (CT) and Memory Space (MS) of the analytical method are lower than those of the numerical method.

Fig. 8 shows that both methods provide a similar SoE trajectory and almost the same optimal controls for the ARTEMIS highway cycles.

6. CONCLUSIONS

In this paper, an analytical approach has been presented and applied to calculate the energy management strategy for a parallel HEV. The results of the comparison show that the analytical method, which is based on analytical models, provides an optimal solution close to the one given by the numerical method, thereby validating the

Cycle	**Strategy**	**FC [L/100km]**	**EL [Wh]**	**CT [ms]**	**MS [Bytes]**
ARTEMIS Highway	Analytical	6.26	**616**	**0.5**	**44**
	Num_1	6.26	**602**	**1.2**	**80**
	Num_2	6.25	**615**	**2**	**530**
ARTEMIS Urban	Analytical	5.28	**195**	**0.5**	**44**
	Num_1	5.30	**192**	**1.2**	**80**
	Num_2	5.24	**193**	**2**	**530**

Table 1. Fuel Consumption, Electric Losses, Computing Time and Memory results

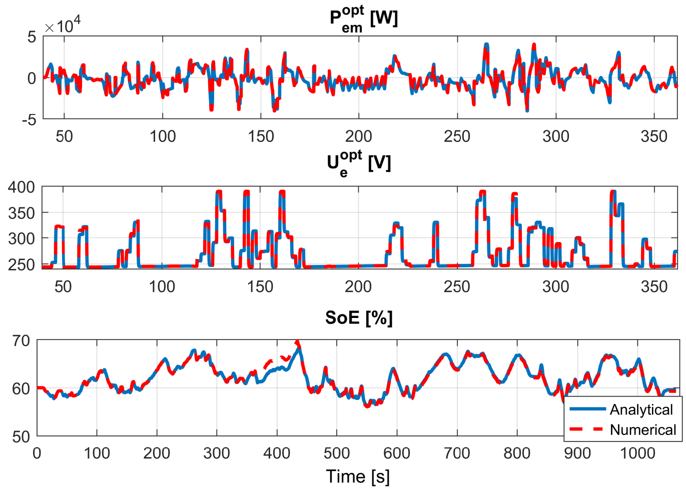

Fig. 8. The optimal controls and the SoE trajectory obtained by the numerical method "Num_2" and the analytical method for the ARTEMIS Highway cycle

approximated generic models. The implementation of the analytical solutions is easier and requires less computing time than the numerical resolution. This encourages their use for embedded optimal control.

As perspectives, the analytical method will be applied to other HEV architectures (serial, serial-parallel), and to more complex configurations (several EM and batteries). This strategy will be implemented for real-time energy management. The robustness analysis will be studied with respect to the parameters of the EM model and those of the engine.

REFERENCES

Ahmadizadeh, P., Mashadi, B., and Lodaya, D. (2017). Energy management of a dual-mode power-split powertrain based on the pontryagin's minimum principle. *IET Intelligent Transport Systems*, 11(9), 561–571.

Ambühl, D., Sundström, O., Sciarretta, A., and Guzzella, L. (2010). Explicit optimal control policy and its practical application for hybrid electric powertrains. *Control engineering practice*, 18(12), 1429–1439.

Asher, Z.D., Baker, D.A., and Bradley, T.H. (2017). Prediction error applied to hybrid electric vehicle optimal fuel economy. *IEEE Transactions on Control Systems Technology*.

Badin, F. (2013). *Hybrid Vehicles*. Technip.

Debert, M., Colin, G., Chamaillard, Y., Mensler, M., Ketfi-cherif, A., and Guzzella, L. (2010). Energy management of a high efficiency hybrid electric automatic transmission. Technical Report 2010-01-1311.

Elbert, P., Nuesch, T., Ritter, A., Murgovski, N., and Guzzella, L. (2014). Engine on/off control for the energy management of a serial hybrid electric bus via convex optimization. *Vehicular Technology, IEEE Transactions on*, 63(8), 3549–3559.

Hadj-Said, S., Colin, G., Ketfi-Cherif, A., and Chamaillard, Y. (2017). Analytical solution for energy management of parallel hybrid electric vehicles. *IFAC-PapersOnLine*, 50(1), 13872–13877.

Johannesson, L., Asbogard, M., and Egardt, B. (2007). Assessing the potential of predictive control for hybrid vehicle powertrains using stochastic dynamic programming. *IEEE Transactions on Intelligent Transportation Systems*, 8(1), 71–83.

Kim, N., Cha, S., and Peng, H. (2011). Optimal control of hybrid electric vehicles based on pontryagin's minimum principle. *Control Systems Technology, IEEE Transactions on*, 19(5), 1279–1287.

Murgovski, N., Johannesson, L., Sjöberg, J., and Egardt, B. (2012). Component sizing of a plug-in hybrid electric powertrain via convex optimization. *Mechatronics*, 22(1), 106–120.

Nüesch, T., Elbert, P., Flankl, M., Onder, C., and Guzzella, L. (2014). Convex optimization for the energy management of hybrid electric vehicles considering engine start and gearshift costs. *Energies*, 7(2), 834–856.

Pérez, L.V., Bossio, G.R., Moitre, D., and García, G.O. (2006). Optimization of power management in an hybrid electric vehicle using dynamic programming. *Mathematics and Computers in Simulation*, 73(1), 244–254.

Pham, T.H., Kessels, J.T.B.A., van den Bosch, P.P.J., and Huisman, R.G.M. (2016). Analytical solution to energy management guaranteeing battery life for hybrid trucks. *IEEE Transactions on Vehicular Technology*, 65(10), 7956–7971.

Rizzoni, G., Guzzella, L., and Baumann, B.M. (1999). Unified modeling of hybrid electric vehicle drivetrains. *IEEE/ASME Transactions on Mechatronics*, 4(3), 246–257.

Serrao, L., Onori, S., and Rizzoni, G. (2009). Ecms as a realization of pontryagin's minimum principle for hev control. In *Proceedings of the American control conference*, 3964–3969.

Stockar, S., Marano, V., Canova, M., Rizzoni, G., and Guzzella, L. (2011). Energy-optimal control of plug-in hybrid electric vehicles for real-world driving cycles. *IEEE Transactions on Vehicular Technology*, 60(7), 2949–2962.

Toshifumi Yamakawa, H.H. (2011). Motor drive control apparatus,vehicle with motor drive control apparatus, and motor drive control method.

Zhang, P., Yan, F., and Du, C. (2015). A comprehensive analysis of energy management strategies for hybrid electric vehicles based on bibliometrics. *Renewable and Sustainable Energy Reviews*, 48, 88–104.